

Random search for a dark resonance

Alexander Holm Kiilerich* and Klaus Mølmer†

Department of Physics and Astronomy, Aarhus University,
Ny Munkegade 120, DK 8000 Aarhus C. Denmark

(Dated: May 17, 2022)

A pair of resonant laser fields can drive a three-level system into a dark state where it ceases to absorb and emit radiation due to destructive interference. We propose a scheme to search for this resonance by randomly changing the frequency of one of the fields each time a fluorescence photon is detected. The longer the system is probed, the more likely the frequency is close to resonance and the system populates the dark state. Due to the correspondingly long waiting times between detection events, the evolution is non-ergodic and the precision of the frequency estimate does not follow from the conventional Cramér-Rao bound of parameter estimation. Instead, a Lévy statistical analysis yields the scaling of the estimation error with time for precision probing of this kind.

Quantum systems can act as sensitive probes and field sensors [1], and since measurements yield random outcomes, the precision by which the value of a physical parameter can be determined follows from a statistical analysis. For N repeated, independent measurements, the estimation error is governed by the Cramér Rao bound [2] and the Fisher information [3], and scales as $1/\sqrt{N}$.

Recent works have addressed the complementary situation of long, continuous measurements on a single quantum system, and recognized that, e.g., photon counting in a fluorescence experiment of duration T is equivalent to $N \propto T$ independent measurements of the waiting time between consecutive detector clicks [4, 5]. The measurement back action of any continuously performed measurement on a quantum system triggers a transient evolution witnessed in the signal correlation functions [6] and if they have finite relaxation time, the estimation error based on the signal mean values and two-time correlations scale as $1/\sqrt{T}$ [6, 7].

In this Letter, we consider the special case where the fluorescence rate of an atomic system vanishes when it is excited by a laser field on exact resonance. Such dark resonances occur in connection with the phenomenon of electromagnetically induced transparency [8, 9], and due to their narrow linewidths, they are sensitive probes of perturbations on the system, see, e.g. [10–12]. As an alternative to a systematic scanning and accumulation of signal at different, discrete laser frequencies, we shall investigate a random search protocol in which the probe laser frequency may, in principle, come arbitrarily close to the dark resonance. That event is witnessed by the complete absence of signal and suggests application of the following adaptive protocol for the duration T of the experiment: {(i) The system is excited at a frequency picked uniformly within a fixed interval, including the resonance; (ii) When a photon is detected, step (i) is repeated with a new random frequency}.

When driven far from the dark resonance, the high scattering rate implies a high probability for an early photon detection and a shift to a different frequency, while for frequencies close to resonance, the photon emission rate

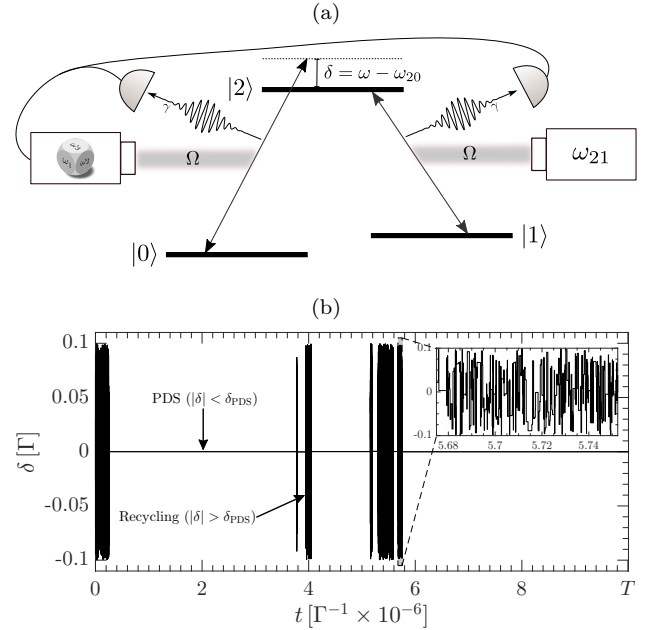


Figure 1. (a) Λ -type system driven by laser fields with Rabi frequency Ω . The $|1\rangle \leftrightarrow |2\rangle$ coupling laser is kept on resonance while the $|0\rangle \leftrightarrow |1\rangle$ coupling laser is detuned by an amount $\delta = \omega - \omega_{20}$, where ω_{20} is the atomic resonance frequency. Both emission channels are monitored by photo detectors, and upon detection in either channel δ is shifted randomly on a uniform interval with $\delta \in [-\delta_{\max}, \delta_{\max}]$. (b) Quantum Monte Carlo simulated trajectory for the detuning δ as a function of time t . The simulation is made with $\Omega = 0.1\Gamma/\sqrt{2}$ and $\delta_{\max} = 0.1\Gamma$ where Γ^{-1} is the excited state lifetime.

is very small, and these frequencies are hence maintained for a long time until the next emission event. Intuitively, we may expect that the longer we probe the atom, the more likely are occurrences of long intervals with laser frequencies very close to the dark resonance. The instantaneous, stochastically tuned laser frequency thus constitutes a good estimate of the atomic transition frequency. Due to the distribution of short, long, and very long time intervals, however, the dynamics is not ergodic, and the Fisher information and Cramér-Rao bound which rely on

asymptotic normality can neither be used to assess the quantitative achievements of the protocol nor to estimate how the error scales with the duration of the experiment.

We show here that the problem is tractable by methods of generalized statistics [13, 14] which have been developed to analyse non-ergodic dynamics in, e.g., animal foraging behaviour [15, 16], human travel patterns [17], earthquake occurrences [18] and financial systems [19, 20]. In quantum physics they have found applications in analysis of anomalous transport properties of quantum arrays [21], and our approach is inspired by and closely follows Bardou *et al.* [22], who apply Lévy statistics to subrecoil laser cooling, mediated by a dark state mechanism. Physical arguments and central equations will be given in the main text and for completeness, details and background will be summarized in the Supplemental Material. While we provide quantitative results and simulations for a specific model, the analysis is general, and we shall return to wider consequences and applications of our results in the final sections of the Letter.

Figure 1a depicts the situation of a Λ -type three-level quantum system interacting with two laser fields with equal coupling strengths. Assume that one field is fixed on resonance, while the other is scanned with a detuning $\delta = \omega - \omega_{20}$ from the exact resonance in the system. The upper level is unstable and decays with equal probabilities into the two low-lying states, which can both be expanded on the dark state $|\psi_{-}\rangle = (|0\rangle - |1\rangle)/\sqrt{2}$ and the bright state $|\psi_{+}\rangle = (|0\rangle + |1\rangle)/\sqrt{2}$. The bright state is coupled to the excited state, and after a short time, the system starting in state $|0\rangle$ or $|1\rangle$ has either undergone excitation and emitted a photon or been effectively projected into the dark state [23]. The dark state has a vanishing excitation rate but for a finite detuning, the phase difference between the laser and the dark state atomic components evolves, and leads to an effective photon emission rate $R(\delta)$. This rate is derived in the Supplemental Material [24] and shown as a function of the detuning δ in Figure 2. If the coupling laser is tuned slightly away from resonance, the effective photo emission rate depends quadratically on the detuning δ , and for a range $|\delta| < \delta_{PDS}$, the system will be trapped for a long time in a pseudo-dark state (PDS). At higher detunings the excitation rate levels off and later falls off when the detuning exceeds $\delta_L \simeq \Gamma$, the excited state linewidth.

A characteristic waiting time between subsequent emissions is $\tau(\delta) = 1/R(\delta)$. Ergodicity relies on the ability to average single trajectories over long times compared to any intrinsic time scale, but since $R(\delta) \rightarrow 0$ we have $\tau(\delta) \rightarrow \infty$ for $\delta \rightarrow 0$, so even a very long time T may be dominated by a single waiting time with $|\delta| < \delta_T$ where $R(\delta_T)T = 1$.

We shall restrict the choice of frequencies to an interval $|\delta| < \delta_{\max}$, containing the resonance, but avoiding the wings of the absorption profile, $\delta_{\max} < \delta_L$. To verify

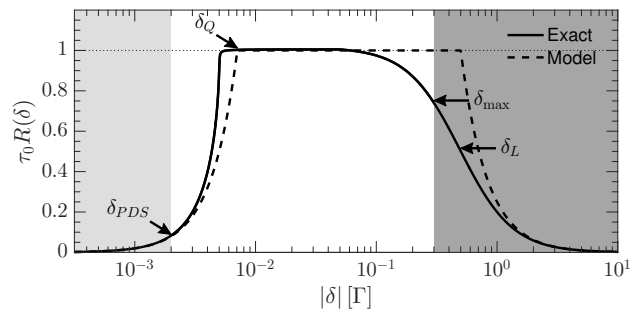


Figure 2. Effective frequency dependent photo emission rate from the dark state $|\psi_{-}\rangle$ shown for $\Omega/\Gamma = 0.1\Gamma/\sqrt{2}$. The full line shows the exact rate and the dashed line our simplified model Eq. (1). Characteristic detunings (see main text) are annotated. The rate is an even function of δ and normalized to a maximum value τ_0^{-1} . The light shaded area is the trapping region and the dark shaded area marks the frequency range not included in the stochastic scan.

the intuition behind the scheme we show in Figure 1b the evolution of the detuning as a function of time as obtained from a Monte-Carlo wave function simulation of the continuous measurements and random frequency jumps. The total duration T is, indeed, dominated by a few long intervals with constant and small detuning, interrupted by brief periods with larger, fluctuating values of δ . The value of the laser frequency at any random time is likely to be very close to the atomic resonance frequency.

While the simulation illustrates the apparent success of such an estimation strategy, a quantitative analysis of its precision and its scaling with T is hampered by the fact that the probability distribution $P(\tau)$ of dwell times τ between detection events has a very long tail, and its mean and variance formally diverge in the interesting regime where $\delta \rightarrow 0$. For such problems, e.g., the sum of N waiting times $T_N = \sum_{i=1}^N \tau^{(i)}$ does not obey the central limit theorem (CLT) and will not converge to a Gaussian distributed variable with a mean value proportional to N . Instead, the increasing probability that a single term attains a very large value and dominates the sum may cause it to scale as a higher power of N . This is the characteristic property of Lévy flights, and $P(T_N)$ is a Lévy-distribution [14].

To obtain analytic predictions for the generic behaviour of our estimation protocol we shall focus on the most significant features and abandon less important details. The variation of the fluorescence rate $R(\delta)$ by an atom occupying the pseudo dark state $|\psi_{-}\rangle$ will thus be approximated by the function

$$R(\delta) = \begin{cases} \tau_0^{-1}(\delta/\delta_Q)^2, & |\delta| < \delta_Q \\ \tau_0^{-1}, & \delta_Q < |\delta| < \delta_L \\ \tau_0^{-1}(\delta_L/\delta)^2, & \delta_L < |\delta|. \end{cases} \quad (1)$$

This simple form of $R(\delta)$, illustrated by the dashed curve in Figure 2, is adequate to represent the very long and

very short waiting times attained for $\delta \simeq 0$ and for larger δ , respectively. The characteristic parameters, yielding the best agreement with the actual rate for the Λ -system illustrated by the solid curve in Figure 2, are derived in [24].

In Figure 1b, we see how the evolution is comprised of two different time scales: In a narrow interval $|\delta| \leq \delta_{\text{PDS}} \leq \delta_{\text{Q}}$, the system occupies the PDS for which the waiting times are of the order $\tau \propto \delta^{-2}$. A single detector click here will with overwhelming probability cause a jump to a detuning $|\delta| \geq \delta_{\text{PDS}}$ where the waiting times are short and many jumps occur before the system returns to the narrow PDS detuning interval. A given trajectory thus consists of a number of trapping intervals $\tau_t^{(1)}, \tau_t^{(2)}, \dots$ interspersed by recycling periods of duration $\tau_r^{(1)}, \tau_r^{(2)}, \dots$ each containing many detection events. The competition between trapping and recycling periods is at the core of our statistical analysis, and the probability distributions $P_t(\tau_t)$ of trapping times τ_t and $P_r(\tau_r)$ of recycling intervals τ_r will suffice to analyse the asymptotic behaviour of our estimation scheme as $T \rightarrow \infty$.

For $P_t(\tau_t)$ we first note that since each detuning in the PDS interval is reached with equal probability, the density of trajectories just returned to the PDS is $\rho(\delta) = \frac{1}{2} \delta_{\text{PDS}}^{-1}$. Upon return with a given δ , the probability of a trapping time τ_t is ascribed by the delay function $w(\tau_t|\delta)$ which can be calculated by a master equation analysis [4, 25]. In the present case we are in the limit of predominantly long waiting times, and $w(\tau_t|\delta)$ is well approximated by a single exponential function, $w(\tau_t|\delta) = R(\delta)^{-1} \exp(-\tau_t R(\delta))$, corresponding to the frequency dependent emission rate $R(\delta)$ which vanishes at $\delta = 0$, cf. Eq.(1).

The distribution $P_t(\tau_t)$ of trapping intervals is now given by integrating $w(\tau_t|\delta)$ over the PDS region with the uniform weight $\rho(\delta)$, and we find for long τ , that

$$P_t(\tau_t) \underset{\text{large } \tau_t}{\simeq} \mu \tau_b^\mu / \tau_t^{1+\mu}, \quad (2)$$

where $\mu = 1/2$, and $\tau_b = \tau_0 \pi (\delta_{\text{PDS}}/\delta_{\text{Q}})^2 / 16$. As anticipated by the arguments above, $P_t(\tau_t)$ decreases very slowly (as $1/\tau_t^{3/2}$) for large values of τ , and we are in the regime where standard Gaussian statistics must be replaced by Lévy statistics.

For a distribution with power law tails such as Eq. (2) all moments $\langle \tau^n \rangle$ for which $n \geq \mu$ diverge. A well-known example is a Cauchy distribution which has $\mu = 1$. The central limit theorem of Gaussian statistics states that for $\mu > 1$ the total time spent in the trapping region $T_N^{(\text{PDS})} = \sum_{i=1}^N \tau_t^{(i)}$ is for large N proportional to the total number of elements, while for $\mu < 1$ any sequence is dominated by rare events and the generalized CLT dictates that asymptotically $T_N^{(\text{PDS})} \propto N^{1/\mu}$. See Supplemental Material [24] for a brief introduction to broad distributions and the generalized CLT.

The behaviour of $R(\delta)$ for large δ determines $P_r(\tau_r)$. When setting up the protocol, we have a choice in the maximum and minimum values allowed in the random selection of δ after each detection event. We assume that a rough prior estimate of the resonance frequency has been obtained, so that the search interval $\delta \in [-\delta_{\text{max}}, \delta_{\text{max}}]$ may be set around $\omega = \omega_{20}$. The symmetry is not of importance since we assume $\delta_{\text{max}} \gg \delta_{\text{PDS}}$. The properties of $P_r(\tau_r)$ depend on the value of δ_{max} compared to the characteristic detunings δ_{Q} and δ_{L} . If $\delta_{\text{Q}} \ll \delta_{\text{max}} < \delta_{\text{L}}$, the high δ rate is given by the plateau in Figure 2 and we obtain a finite mean value $\langle \tau_r \rangle = \tau_0 (\delta_{\text{max}}/\delta_{\text{PDS}})$ [24], implying that $T_N^{(\text{REC})} = \sum_{i=1}^N \tau_r^{(i)}$ grows linearly with N . For simplicity we restrict our attention to this case and defer discussion of the case with $\delta_{\text{max}} > \delta_{\text{L}}$ to our concluding remarks.

This result already provides qualitative insight regarding the asymptotic achievements of our estimation scheme at large times T (large N). For $\delta_{\text{max}} < \delta_{\text{L}}$, $T_N^{(\text{PDS})} \propto N^2$ dominates over $T_N^{(\text{REC})} \propto N$, and we expect trajectories to spend most of the time in the PDS. In fact, the time averaged proportion of time in the PDS is given by $f_T(T) = T_N^{(\text{PDS})} / (T_N^{(\text{PDS})} + T_N^{(\text{REC})})$, which for long times T can be written $f_T(T) = 1 - \xi (\langle \tau_r \rangle / \tau_b) T^{(\mu-1)}$ [24]. This reveals a time-averaged non-PDS proportion decreasing as $1/\sqrt{T}$, but contrary to ergodic processes with Gaussian statistics it continues to fluctuate, via the Lévy increment ξ , even in the high T limit.

To assess the expected estimation achievements we address the ensemble averaged trapped proportion which as derived in [24] is given by

$$f_E(T) \simeq 1 - \frac{\sin(\pi\mu)}{\pi} \frac{\langle \tau_r \rangle}{\tau_b^\mu T^{1-\mu}}, \quad (3)$$

where we see the same scaling with time T , but without fluctuations. Equation (3) expresses the probability as a function of time that the laser frequency and hence the parameter estimate is within δ_{PDS} of the true resonance frequency, while with a probability $1 - f_E(T)$ the frequency resides, at the time T , in the recycling region, and will not be a good estimator of the resonance frequency. The fact that $f_E(T)$ converges to unity for large T hence signifies that the random search is a successful estimation scheme. In Figure 3 we show how $f_E(T)$ matches the ensemble average of trajectories such as the one in Figure 1b for large times, $T \gtrsim 10^6 \Gamma^{-1}$.

To address the sensitivity of the random search we consider the distribution $\mathcal{P}(\delta, T)$ of trajectories with $|\delta| < \delta_{\text{PDS}}$. This also follows from the Lévy statistical analysis [24]. Generally $\mathcal{P}(\delta, T)$ can be factorized as $\mathcal{P}(\delta, T) = h(T)G(q)$, where $h(T)$ is the time-dependent height of the distribution and $G(q)$, where $q = \delta/\delta_T$, is a form factor. It is a signature of the broken ergodicity that $\mathcal{P}(\delta, T)$ depends explicitly on T and does not approach a stationary form even for very

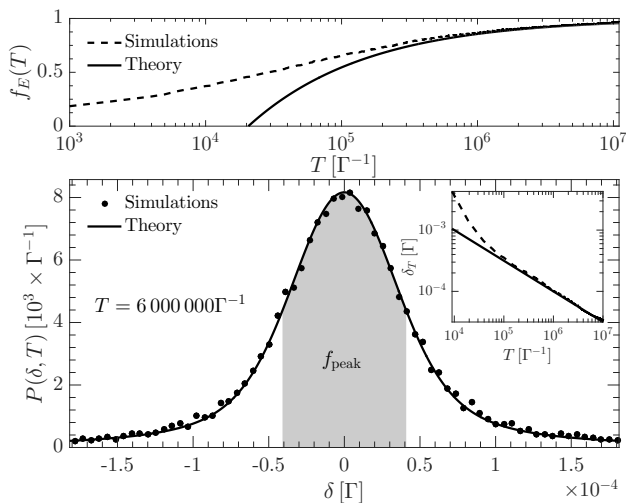


Figure 3. Top: Proportion of trapped trajectories Eq. (3) (with $\delta_{\text{PDS}} = 0.01\Gamma$) as a function of time. Dashed line depicts simulated data from a quantum jump simulation of 20 000 trajectories with the same parameters as in Figure 1b. It matches the statistical model (full line) for (very) large times. Bottom: Distribution of the detuning δ after a long time $T = 6 \times 10^6 \Gamma^{-1}$. Dots show simulated data, the full line shows the theoretical result of our statistical analysis and the shaded area marks the fraction with $|\delta| \leq \delta_T$. The inset shows how the characteristic width δ_T of the distribution scales as $T^{-1/2}$ and matches the model for times larger than $\simeq 10^5 \Gamma^{-1}$.

long times. We find $h(T) = (\tau_{\text{PDS}}/\tau_b)^\mu \sin(\pi\mu)/(\pi\mu\delta_T)$, where $\tau_{\text{PDS}} = 1/R(\delta_{\text{PDS}})$. A general expression for the form factor is given in the Supplemental Material [24]. It depends only on the value of μ , and for $\mu = 1/2$ it may be expressed as $G(q) = D(q)/q$, where $D(q)$ is the Dawson function. The tails of $G(q)$ are Lorentzian $\sim 1/2q^2$ and much wider than those of a Gaussian while its maximum is flat compared to a Lorentzian.

The important detuning scale is, as anticipated, given by $\delta_T = \delta_Q(\tau_0/T)^\mu$. For the height this implies that $h(T) \propto T^\mu$, and the FWHM of $G(q)$ is $w(T) \simeq q_w \delta_T \propto T^{-\mu}$, where for $\mu = 1/2$ we find numerically $q_w \simeq 2.13$. Since the distribution has long tails, we define the fraction $f_{\text{peak}} = \int_{-\delta_T}^{\delta_T} d\delta \mathcal{P}(\delta, T)$ of occurrences of final detunings in the characteristic range $|\delta| < \delta_T$, as a measure for the parameter estimation sensitivity and we find $f_{\text{peak}} \simeq 0.59$ independently of T . This directly shows that asymptotically a constant part of the trajectories are within $\delta_T \propto T^{-\mu}$ of the true resonance frequency. We note that the sensitivity does not depend on the values of δ_{max} and δ_{PDS} as long as $\delta_{\text{PDS}} \ll \delta_{\text{max}} < \delta_L$ is fulfilled. For the Λ -system with $\mu = 1/2$ we hence find a $1/\sqrt{T}$ scaling of the sensitivity in our estimation protocol. We note that 59% of the distribution within δ_T corresponds to $\simeq 0.82$ sigma confidence level had $\mathcal{P}(\delta, T)$ been a normal distribution.

In Figure 3 we show how the ensemble obtained from

simulations until $T = 6 \times 10^6 \Gamma^{-1}$ is well represented by $\mathcal{P}(\delta, T)$. The inset shows the consistency of the theoretical result for δ_T with numerical results obtained directly from the sampled $\mathcal{P}(\delta, T)$ as a function of time.

We have shown that under certain restrictions our estimation scheme is successful, but it remains to be seen if it outperforms standard spectroscopy methods in the same settings. A typical way to determine a resonance frequency is by observing fluorescence as the laser frequency is systematically scanned over the relevant frequencies with equal time at each point. The spectrum is reconstructed from the integrated fluorescence signal at each frequency. Such a scheme lends itself to a standard analysis relying on the CRB, which reveals an uncertainty scaling as $1/\sqrt{T}$ [24]. A comparison shows that for the parameters used in Figure 1b, our stochastic scan proves superior to the systematic scan if we search an interval $[-\delta_{\text{max}}, \delta_{\text{max}}]$ with $\delta_{\text{max}} > 0.09\Gamma$, i.e. as long as the resonance is not a-priori known to very high precision.

Finally, while we presented the scheme for a driven Λ -system and restricted our attention to a rate $R(\delta)$ with a quadratic dip around $\delta = 0$ and a flat plateau for large $\delta \simeq \delta_{\text{max}}$, the arguments applied are general, and the statistical methods apply equally well to other systems. For example, different forms of $R(\delta) \propto \delta^\alpha$ for $\delta \simeq 0$ will lead to different values of $\mu = 1/\alpha$ which will, in turn, imply different scaling with time of the sensitivity as quantified by $\delta_T \propto T^{-\mu}$. For example, a variant of the presented scheme may apply Raman pulses rather than continuous illumination. It can be shown that e.g. a sequence of Blackman pulses [26] yield an excitation probability characterized by $\mu = 1/4$, while square pulses lead to $\mu = 1/2$ [27].

If ω_{20} is only known to a precision of $\lesssim \Gamma$, δ_{max} must be chosen bigger than δ_L . In this case, the rate decreases as $1/\delta^2$ in the recycling region leading to recycling times of order $\sim \delta^2$, and there is a risk that trajectories will be trapped far away from the resonance. The return times are then also described by anomalous statistics and $P_r(\tau_r)$ is of the form Eq. (2) with $\mu_r < 1$. The actual value of μ_r depends on the detailed frequency shifting protocol. If δ is restricted to jump to a vicinity of the current value one finds $\mu_r = 1/4$ [28] and $T_N^{(\text{REC})} \propto N^4$. Our scheme then fails asymptotically as $f_E(T) \rightarrow 0$ for large T . If, on the other hand, the laser frequency is shifted uniformly on the search interval, the exact zero at $\delta = 0$ dominates the asymptotic zero as $|\delta| \rightarrow \infty$, and the trajectories will in fact converge (albeit slower) to the PDS.

We have in this Letter proposed to locate the absorption zero of a dark resonance by a random frequency search protocol. Due to the non-ergodic behavior of the system, methods from Lévy statistics were employed to assess the asymptotic spectroscopic sensitivity of the method. For the actual example of a driven Λ -type system, our method compares favourably with the Cramér-

Rao bound of a conventional frequency scan. Metrology protocols have been proposed, which feature similar feedback and adaptive elements, and which show convergence faster than $1/\sqrt{T}$ or $1/\sqrt{N}$ where N quantifies the amount of physical resources, see e.g. [1, 29–31]. Since adaptive schemes may generally induce non-ergodic dynamics, we believe that our theoretical analysis will be relevant in the characterization of a number of such protocols where standard statistical analyses are inadequate.

The authors acknowledge financial support from the Villum Foundation. A. H. K. further acknowledges support from the Danish Ministry of Higher Education and Science.

-
- [1] V. Giovannetti, S. Lloyd, and L. Maccone, “Quantum metrology,” *Phys. Rev. Lett.* **96**, 010401 (2006).
- [2] H. Cramér, “Mathematical methods of statistics,” Princeton mathematical series No. 9 (Princeton University Press, Princeton, 1954).
- [3] R. A. Fisher, “On the mathematical foundations of theoretical statistics,” *Philosophical Transactions of the Royal Society A* **222**, 309–368 (1922).
- [4] A. H. Kiilerich and K. Mølmer, “Estimation of atomic interaction parameters by photon counting,” *Phys. Rev. A* **89**, 052110 (2014).
- [5] A. H. Kiilerich and K. Mølmer, “Parameter estimation by multichannel photon counting,” *Phys. Rev. A* **91**, 012119 (2015).
- [6] A. H. Kiilerich and K. Mølmer, “Bayesian parameter estimation by continuous homodyne detection,” *Phys. Rev. A* **94**, 032103 (2016).
- [7] D. Burgarth, V. Giovannetti, A. N. Kato, and K. Yuasa, “Quantum estimation via sequential measurements,” *New Journal of Physics* **17**, 113055 (2015).
- [8] H. R. Gray, R. M. Whitley, and C. R. Stroud, “Coherent trapping of atomic populations,” *Opt. Lett.* **3**, 218–220 (1978).
- [9] K.-J. Boller, A. Imamoglu, and S. E. Harris, “Observation of electromagnetically induced transparency,” *Phys. Rev. Lett.* **66**, 2593–2596 (1991).
- [10] A. Nagel, L. Graf, A. Naumov, E. Mariotti, V. Biancalana, D. Meschede, and R. Wynands, “Experimental realization of coherent dark-state magnetometers,” *Europhys. Lett.* **44**, 31 (1998).
- [11] C. L. Holloway, J. A. Gordon, S. Jefferts, A. Schwarzkopf, D. A. Anderson, S. A. Miller, N. Thaicharoen, and G. Raithel, “Broadband rydberg atom-based electric-field probe for si-traceable, self-calibrated measurements,” *IEEE Transactions on Antennas and Propagation* **62**, 6169–6182 (2014).
- [12] M. Stähler, S. Knappe, C. Affolderbach, W. Kemp, and R. Wynands, “Picotesla magnetometry with coherent dark states,” *Europhys. Lett.* **54**, 323 (2001).
- [13] P. Lévy, “Théorie de l’addition des variables aléatoires, 2nd edn.” (Gauthier-Villars, Paris, 2010).
- [14] J.-P. Bouchaud and A. Georges, “Anomalous diffusion in disordered media: Statistical mechanisms, models and physical applications,” *Physics reports* **195**, 127–293 (1990).
- [15] D. W. Sims, E. J. Southall, N. E. Humphries, G. C. Hays, C. J. A. Bradshaw, J. W. Pitchford, A. James, M. Z. Ahmed, A. S. Brierley, M. A. Hindell, *et al.*, “Scaling laws of marine predator search behaviour,” *Nature* **451**, 1098–1102 (2008).
- [16] G. M. Viswanathan, S. V. Buldyrev, S. Havlin, M. G. E. Da Luz, E. P. Raposo, and H. E. Stanley, “Optimizing the success of random searches,” *Nature* **401**, 911–914 (1999).
- [17] D. Brockmann, L. Hufnagel, and T. Geisel, “The scaling laws of human travel,” *Nature* **439**, 462–465 (2006).
- [18] Á. Corral, “Universal earthquake-occurrence jumps, correlations with time, and anomalous diffusion,” *Phys. Rev. Lett.* **97**, 178501 (2006).
- [19] B. Mandelbrot, “The variation of certain speculative prices,” *The Journal of Business* **36** (1963).
- [20] R. N. Mantegna and H. E. Stanley, “Turbulence and financial markets,” *Nature* **383**, 587–588 (1996).
- [21] D. S. Novikov, M. Drndic, L. S. Levitov, M. A. Kastner, M. V. Jarosz, and M. G. Bawendi, “Lévy statistics and anomalous transport in quantum-dot arrays,” *Phys. Rev. B* **72**, 075309 (2005).
- [22] F. Bardou, J.-P. Bouchaud, O. Emile, A. Aspect, and C. Cohen-Tannoudji, “Subrecoil laser cooling and Lévy flights,” *Phys. Rev. Lett.* **72**, 203–206 (1994).
- [23] J. Dalibard, Y. Castin, and K. Mølmer, “Wave-function approach to dissipative processes in quantum optics,” *Phys. Rev. Lett.* **68**, 580–583 (1992).
- [24] See Supplemental Material at [URL will be inserted by publisher] for background and derivations of central results.
- [25] H. Carmichael, “An Open Systems Approach to Quantum Optics - Lectures Presented at the Université Libre de Bruxelles October 28 to November 4, 1991,” (Springer, Berlin Heidelberg, 1993).
- [26] F. J. Harris, “On the use of windows for harmonic analysis with the discrete fourier transform,” *Proceedings of the IEEE* **66**, 51–83 (1978).
- [27] J. Reichel, F. Bardou, M. Ben Dahan, E. Peik, S. Rand, C. Salomon, and C. Cohen-Tannoudji, “Raman cooling of Cesium below 3 nK: New approach inspired by Lévy flight statistics,” *Phys. Rev. Lett.* **75**, 4575–4578 (1995).
- [28] F. Bardou, J.-P. Bouchaud, A. Aspect, and C. Cohen-Tannoudji, “Lévy Statistics and Laser Cooling,” (Cambridge University Press, Cambridge, 2002).
- [29] B. L. Higgins, D. W. Berry, S. D. Bartlett, H. M. Wiseman, and G. J. Pryde, “Entanglement-free Heisenberg-limited phase estimation,” *Nature* **450**, 393–396 (2007).
- [30] M. Mehboudi and L. A. Correa, “Achieving sub-shot-noise sensing at finite temperatures,” arXiv:1604.06400v2 (2016).
- [31] L. A. Clark, A. Stokes, and A. Beige, “Quantum-enhanced metrology with the single-mode coherent states of an optical cavity inside a quantum feedback loop,” *Phys. Rev. A* **94**, 023840 (2016).

Supplemental Materials: Random search for a dark resonance

Here we provide additional material and derivations of central results in the main text.

EFFECTIVE EMISSION RATE FOR A LASER DRIVEN Λ -SYSTEM

The laser driven Λ -system in Figure 1a of the main text is described by the Hamiltonian

$$\hat{H} = \delta |0\rangle \langle 0| + \frac{\Omega}{2} (|2\rangle \langle 0| + |0\rangle \langle 2|) + \frac{\Omega}{2} (|2\rangle \langle 1| + |1\rangle \langle 2|), \quad (\text{S1})$$

with laser atom detuning δ and Rabi frequency Ω .

The evolution of the density matrix ρ of the unobserved system is given by the master equation $d\rho/dt = L[\rho]$, where the Liouvillian superoperator is defined by ($\hbar = 1$)

$$L[\rho] = -i[\hat{H}, \rho] + \sum_i \left(\hat{c}_i \rho \hat{c}_i^\dagger - \frac{1}{2} \left\{ \hat{c}_i^\dagger \hat{c}_i, \rho \right\} \right). \quad (\text{S2})$$

Here the excited state spontaneous decay with rate Γ is represented by the relaxation operators $\hat{c}_0 = \sqrt{\Gamma/2} |2\rangle \langle 0|$ and $\hat{c}_1 = \sqrt{\Gamma/2} |2\rangle \langle 1|$. The unobserved system relaxes to a steady state ρ_{ss} with $L[\rho_{\text{ss}}] = 0$ from which follows the average properties of the emitted radiation. In particular, the average fluorescence rate is given by $\tilde{R}(\delta) = \sum_i \text{Tr} \left(\hat{c}_i^\dagger \hat{c}_i \rho_{\text{ss}} \right)$ where $i = 0, 1$, and the quantum regression theorem yields Glauber's correlation function [S5] for two photo emissions in channel i separated by a time τ ,

$$G_i^{(2)}(\tau) = \text{Tr} \left(\hat{c}_i^\dagger \hat{c}_i e^{L\tau} \left[\hat{c}_i \rho_{\text{ss}} \hat{c}_i^\dagger \right] \right). \quad (\text{S3})$$

The master equation can be unravelled into stochastic evolution corresponding to the random measurement back action on the system due to detection of the emitted radiation by photon detectors. Whenever a photon is detected, the system jumps to the corresponding ground state, $|\psi\rangle \rightarrow \hat{c}_i |\psi\rangle / \sqrt{\langle \psi | \hat{c}_i^\dagger \hat{c}_i | \psi \rangle}$, while between photo detections the evolution of the (unnormalized) state $|\tilde{\psi}\rangle$ is governed by an effective Hamiltonian,

$$\hat{H}_{\text{eff}} = \hat{H} - \frac{i}{2} \sum_i \hat{c}_i^\dagger \hat{c}_i, \quad (\text{S4})$$

where the imaginary term represents the decay of the excited state. The eigenstates of \hat{H}_{eff} , $|\psi_j\rangle$ with eigenvalues λ_j represent decaying modes with decay rates $\Gamma_j = -2\text{Im}(\lambda_j)$. For weak driving, the largest of these rates is almost equal to Γ and the corresponding eigenstate is close to the bare atomic excited state, i.e., it has negligible statistical weight $w_j^{(n)} = |\langle n | \psi_j \rangle|^2$ on the atomic

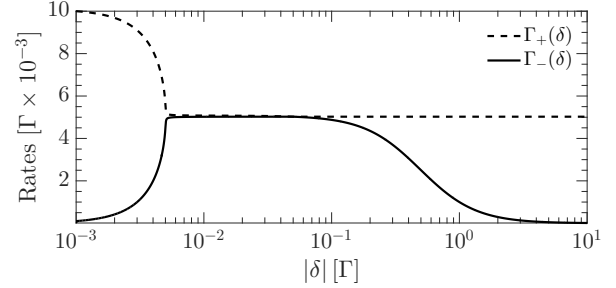


Figure S1. Frequency dependent effective emission rates from the bright $|\psi_+\rangle$ and dark $|\psi_-\rangle$ state superpositions of the two ground states of a Λ -type system. The rates are even functions of δ and results are shown for $\Omega = 0.1\Gamma/\sqrt{2}$.

ground states ($n = 0, 1$). The two smallest rates Γ_- and Γ_+ , on the other hand, are associated with the ground states, and hence constitute the effective fluorescence rate right after a detector click. Their dependence on the detuning δ is shown in Figure S1. Close to resonance $\Gamma_-(\delta)$ tends quadratically to zero, while $\Gamma_+(\delta)$ increases equivalently. This is because $\Gamma_-(\delta \simeq 0) \simeq 0$ corresponds to the dark state superposition $|\psi_-\rangle = (|0\rangle - |1\rangle)/\sqrt{2}$ while $\Gamma_+(\delta \simeq 0) \simeq 2\Omega^2/\Gamma$ is the rate of excitation and emission from the bright state linear combination $|\psi_+\rangle = (|0\rangle + |1\rangle)/\sqrt{2}$.

Upon photo detection, the atom may with probability $w_+^{(0,1)} \simeq 1/2$ continue to fluoresce at a rate $\Gamma_+(\delta)$, and hence quickly reemit, but it may also with a probability $w_-^{(0,1)} \simeq 1/2$ continue to fluoresce at a rate $\Gamma_-(\delta)$ corresponding to the pseudo dark state. The frequency dependent emission rate leading to non-ergodic dynamics close to resonance is thus given by $R(\delta) = \Gamma_-(\delta)$.

Our Lévy statistical analysis relies on the overall rather than the detailed shape of the emission rate from the ground states. In this spirit we note that the fluorescence rate $\Gamma_-(\delta)$ as a function of the detuning is characterized by a dip with quadratic variation around $\delta = 0$ due to the dark state, a plateau where the rate is constant, and a tail where the decay follows a Lorentzian line shape due to off-resonant scattering. We hence approximate the rate by

$$R(\delta) = \begin{cases} \tau_0^{-1}(\delta/\delta_Q)^2, & |\delta| < \delta_Q \\ \tau_0^{-1}, & \delta_Q < |\delta| < \delta_L \\ \tau_0^{-1}(\delta_L/\delta)^2, & \delta_L < |\delta|. \end{cases} \quad (\text{S5})$$

where the characteristic parameters are identified by matching the plateau to the maximum of $\Gamma^{(-)}(\delta)$, and requiring that $R(\delta)$ represents the exact form in the limits $\delta \simeq 0$ and $\delta \gg 0$. Though not a necessity for our analysis we assume for simplicity that the coupling is weak ($\Omega \ll \Gamma$). We then find by applying second order

perturbation theory that

$$\begin{aligned}\tau_0 &= \frac{\Gamma}{\Omega^2} \\ \delta_Q &= \sqrt{2} \frac{\Omega^2}{\Gamma} \\ \delta_L &= \frac{\Gamma}{2}.\end{aligned}\quad (\text{S6})$$

The approximation Eq. (S5) is compared to the exact rate in Figure 2 of the main text.

BROAD DISTRIBUTIONS AND LÉVY STATISTICS

In this section we give a brief introduction to 'broad distributions' decaying slowly at large deviations. We will focus on the typical cases of power law decays. Let τ be a positive random variable distributed for large values according to

$$P(\tau) \underset{\text{large } \tau}{\simeq} \frac{\mu \tau_b^\mu}{\tau^{1+\mu}}, \quad (\text{S7})$$

where the exponent μ determines the decay of the tail towards zero. Normalizability requires $\mu > 0$ and all moments $\langle \tau^n \rangle$ for which $n \geq \mu$ diverge.

The central limit theorem (CLT) concerns the asymptotic behaviour of the sum T_N of N independent realizations of the probability distribution $P(\tau)$,

$$T_N = \sum_{i=1}^N \tau_i, \quad (\text{S8})$$

independent of the detailed shape of $P(\tau)$.

For $\mu > 2$ both the mean $\langle \tau \rangle$ and variance σ^2 of τ are finite, and defining a random variable ϵ such that

$$T_N = \langle \tau \rangle N + \epsilon \sigma \sqrt{N}, \quad (\text{S9})$$

the normal CLT ensures that for large N , ϵ is a Gaussian random variable with zero mean and unit variance. I.e. T_N is normally distributed and $T_N \rightarrow \langle \tau \rangle N$ for large N .

For $\mu < 2$ the variance of τ is formally infinite, and the normal CLT does not apply. Instead a generalized CLT has been proven by Lévy and Gnedenko [S13, S14]. If $1 < \mu < 2$ the mean value of τ is finite and by defining the Lévy increment ξ such that

$$T_N = \langle \tau \rangle N + \xi \tau_b N^{1/\mu}, \quad (\text{S10})$$

the generalized CLT states that ξ is a random variable of order one distributed according to the completely asymmetric Lévy distribution $L_\mu(\xi)$ which only depends on the value of μ . Notice, however, that we still have $T_N \rightarrow \langle \tau \rangle N$ for large N .

The most interesting case in the present work is $\mu < 1$ where even the mean of τ is undefined. Then Eq. (S10) becomes

$$T_N = \xi \tau_b N^{1/\mu}, \quad (\text{S11})$$

where ξ is distributed as above, and we note that the sum Eq. (S8) does no longer scale proportionally with the number of terms, but is rather dominated by a few single terms.

RECYCLING TIME DISTRIBUTION

Here we address the temporal dynamics and derive the probability distribution $P_r(\tau_r)$ of the recycling time intervals τ_r .

We introduce first the probability $P_1(k)$ that the detuning returns to the PDS (defined in the main text) for the first time exactly k photon detection events after leaving the PDS. Notice that $P_1(k)$ relates to the number of jumps and *not* to the duration τ_r of the time spent outside the PDS. The probability $P_{\text{trap}}(n)$ that the system occupies the PDS after the n^{th} detection event can be written as a sum over probabilities of already being trapped after n' events with probability $P_{\text{trap}}(n')$, leaving the PDS at $n' + 1$ (which occurs with unit probability since $\delta_{\text{PDS}} \ll \delta_{\text{max}}$) and returning after an additional $n - n'$ steps with a probability $P_1(n - n')$,

$$P_{\text{trap}}(n) = P_1(n) + \sum_{n'=0}^{n-1} P_{\text{trap}}(n') P_1(n - n'), \quad (\text{S12})$$

where the first term accounts for a first return at n without any prior returns. We assume an initial detuning in the recycling region, and we have extended the summation limits to $n' = 0$ and $n' = n$ which is justified since $P_{\text{trap}}(0) = 0$ and $P_1(0) = 0$.

The sum constitutes a convolution product, and we introduce the discrete Laplace transform (moment-generating function),

$$\mathcal{L}_d P(s) = \sum_{n=0}^{\infty} e^{-sn} P(n) \quad (\text{S13})$$

realizing the relation between $P_1(n)$ and $P_{\text{trap}}(n)$,

$$\mathcal{L}_d P_1(s) = \frac{\mathcal{L}_d P_{\text{trap}}(s)}{1 + \mathcal{L}_d P_{\text{trap}}(s)}. \quad (\text{S14})$$

This result is independent of any specific frequency shifting protocol.

The main text investigates the case where after each detection event the detuning explores the interval $\delta \in [-\delta_{\text{max}}, \delta_{\text{max}}]$ in a uniform manner. In such settings $P_{\text{trap}}(n)$ has a constant value

$$P_{\text{trap}}(n) = \frac{\delta_{\text{PDS}}}{\delta_{\text{max}}}, \quad (\text{S15})$$

and Eq. (S14) yields

$$\mathcal{L}_d P_1(s) = 1 - \frac{\delta_{\max}}{\delta_{\text{PDS}}} s. \quad (\text{S16})$$

Since $\mathcal{L}_d P_1(s)$ is a moment-generating function this implies that the average number of steps before the first return is finite and given by

$$\langle n \rangle = \frac{\delta_{\max}}{\delta_{\text{PDS}}}. \quad (\text{S17})$$

The temporal duration of each step depends on the emission rate in the recycling region. In the main text we focus on the case $\delta_Q \ll \delta_{\max} < \delta_L$, where the recycling region is characterized by a frequency independent rate, $R(\delta) = 1/\tau_0$, and the average time τ_0 between two jumps is finite. The average first return time is then simply

$$\langle \tau_r \rangle = \langle n \rangle \tau_0. \quad (\text{S18})$$

The finite mean value implies that the recycling times τ_r follow normal statistics. In fact, it can be shown that the tail of $P_r(\tau_r)$ follows an exponential law [S9].

If the frequency shifting is performed as an unconfined standard random walk Eq. (S14) still applies and leads to a first return distribution with a power law tail

$$P_1(n) \underset{\text{large } n}{\simeq} \frac{1}{2\sqrt{2\pi}} \frac{\Delta\delta}{\delta_{\text{PDS}}} \frac{1}{n^{3/2}} \quad (\text{S19})$$

with $\Delta\delta$ the average step size [S28]. In this case $\langle n \rangle$ diverges. The corresponding statistical behaviour of the recycling times τ_r is dominated by trapping in effective dark states at high δ where, by Eq. (S5), $R(\delta) \propto 1/\delta^2$. One finds [S28] that $P_r(\tau_r)$ then follows Eq. (S7) with $\mu_r = 1/4$ and $\tau_{r,b} = \tau_0(\Delta\delta)^6/(\delta_{\text{PDS}}^4 \delta_L^2)$, and that the recycling process is dominated by very long time intervals.

PROPORTION OF TRAPPED TRAJECTORIES

Here we derive the proportion of trajectories that will asymptotically for long times be trapped in the PDS with $|\delta| < \delta_{\text{PDS}}$. Due to the non-ergodic dynamics, the time average, unlike the ensemble average results, retains a stochastic contribution even in the long time limit.

The alternation between trapping and recycling periods defines a renewal process [S3], and we introduce first the probability density functions $S_R(t)$ of returning to the PDS region at time t independent of the number of previous return points and $S_D(t)$ for departing at time t independent of previous departure points. I.e. $S_R(t)dt$ ($S_D(t)dt$) is the probability of entering (departing) the PDS region in $[t, t + dt]$. The densities can be expressed in terms of each other and the trapping and recycling time distributions. For an initially un-trapped trajectory, we have

$$S_R(t) = P_r(t) + \int_0^t dt' S_D(t') P_r(t - t'), \quad (\text{S20})$$

where the first term accounts for the probability of being trapped exactly at t and the second the case of escaping at $t' \in [0, t]$ and returning at t . Similarly

$$S_D(t) = \int_0^t dt' S_R(t') P_t(t - t'). \quad (\text{S21})$$

The integrals in the expressions (S20,S21) form convolution products, so performing Laplace transforms, $\mathcal{L}g(s) = \int_0^\infty dt g(t)e^{-st}$, and eliminating $\mathcal{L}S_D(s)$, we find

$$\mathcal{L}S_R(s) = \frac{\mathcal{L}P_r(s)}{1 - \mathcal{L}P(s)\mathcal{L}P_r(s)}. \quad (\text{S22})$$

The ensemble average trapped proportion at time T can be written as an integral over time t' of the probability that the system entered the trap at time t' multiplied by the probability $\psi(T - t')$ that the system remained in the trap until times later than T ,

$$f_E = \int_0^T dt' S_R(t') \psi(T - t'). \quad (\text{S23})$$

Note that $\psi(T - t')$ is itself an integral over the distribution $P_t(T - t')$ of trapping times,

$$\psi(\tau) = \int_\tau^\infty d\tau' P_t(\tau').$$

The Laplace transform of the convolution Eq. (S23) is

$$\mathcal{L}f_E(s) = \mathcal{L}S_R(s)\mathcal{L}\psi(s), \quad (\text{S24})$$

with $\mathcal{L}\psi(s) = (1 - \mathcal{L}P(s))/s$. Inserting Eq. (S22) we thus reach our final expression for the Laplace transform of the trapped proportion,

$$\mathcal{L}f_E(s) = \frac{\mathcal{L}P_r(s)}{1 - \mathcal{L}P_t(s)\mathcal{L}P_r(s)} \frac{1 - \mathcal{L}P_t(s)}{s}, \quad (\text{S25})$$

revealing

$$f_E(T) = \int_0^T dt [S_R(t) - S_E(t)], \quad (\text{S26})$$

which is very sensible.

With $\mathcal{L}f_E(s)$ expressed in terms of the trapping and recycling time distributions we may apply our statistical model. A small s expansion (high τ_t) of the Laplace transform of $P_t(\tau_t)$ as given in Eq. (2) of the main text yields to first order [S28]

$$\mathcal{L}P_t(s) \simeq 1 - \Gamma(1 - \mu)(s\tau_b)^\mu, \quad (\text{S27})$$

where $\Gamma(x)$ is the Gamma-function. For the recycling distribution we focus on the case $\delta_{\max} < \delta_L$, where the mean recycling time is finite so that

$$\mathcal{L}P_r(s) = 1 - s \langle \tau_r \rangle \quad (\text{S28})$$

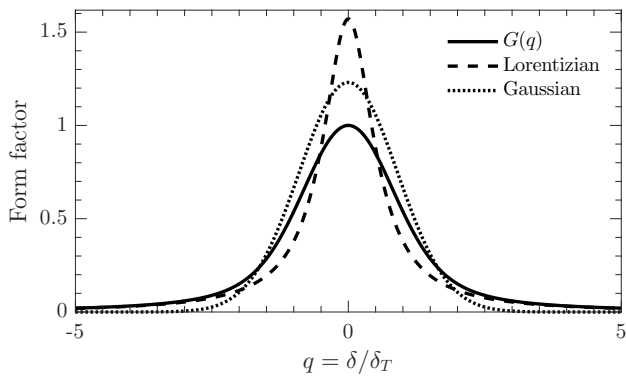


Figure S2. The form factor $G(q)$ Eq. (S35) of $\mathcal{P}(\delta, T)$ is compared to a Lorentzian with the same tails ($\propto 1/2q^2$), and a Gaussian with the same FWHM (2.13). All distributions are normalized to an area $\pi^{3/2}/2$.

for small s . Then by Eq. (S25)

$$\mathcal{L}f_E(s) = \frac{1}{s} - \frac{\langle \tau_r \rangle}{\Gamma(1-\mu)(s\tau_b)^\mu}, \quad (\text{S29})$$

and one can finally show that asymptotically as $T \rightarrow \infty$ the inverse transform gives

$$f_E(T) \simeq 1 - \frac{\sin(\pi\mu)}{\pi} \frac{\langle \tau_r \rangle}{\tau_b^\mu T^{1-\mu}}. \quad (\text{S30})$$

For a discussion of cases where $\delta_{\max} > \delta_L$, the reader is referred to [S28].

ASYMPTOTIC FREQUENCY DISTRIBUTION

The asymptotic proportion of trajectories with $|\delta| < \delta_{\text{PDS}}$ is given by $f_E(T)$. The asymptotic distribution $\mathcal{P}(\delta, T)$ of this proportion is given by integrating the probability of entering the trap at a time t' with a given δ and not leaving before the final time T ,

$$\mathcal{P}(\delta, T) = \rho(\delta) \int_0^T dt' S_R(t') \phi(T - t'|\delta), \quad (\text{S31})$$

where $\rho(\delta) = 1/2\delta_{\text{PDS}}$ is normalized, so $f_E(T) = \int_{-\delta_{\text{PDS}}}^{\delta_{\text{PDS}}} d\delta \mathcal{P}(\delta, T)$, and we define the probability to leave the trap after a time τ conditioned on the value of δ ,

$$\phi(\tau|\delta) = \int_\tau^\infty d\tau' P_t(\tau'|\delta). \quad (\text{S32})$$

As it turns out, the time-dependent distribution of frequencies $\delta \leq \delta_{\text{PDS}}$ within the trap is self-similar for different times and can in general be factorized as

$$\mathcal{P}(\delta, T) = h(T)G(q). \quad (\text{S33})$$

We restrict our attention to the case $\delta_{\max} < \delta_L$ with infinite average trapping time and finite recycling times,

and refer to [S28] for derivations when the recycling is also non-ergodic. From Eq. (S22) and Eq. (S27) it follows that the small s expansion of the Laplace transform of the renewal density function is $\mathcal{L}S_R(s) = (s\tau_b)^{-\mu}/\Gamma(1-\mu)$, so that for large times $S_R(t) \simeq \sin(\pi\mu)\tau_b^{-\mu}t^{\mu-1}/\pi$. One finds then the height of the distribution,

$$h(T) = \left(\frac{\tau_{\text{PDS}}}{\tau_b} \right)^\mu \frac{\sin(\pi\mu)}{\pi\mu\delta_T}. \quad (\text{S34})$$

The form factor is defined as a function of $q = \delta/\delta_T$ as

$$G(q) = \mu \int_0^1 du u^{\mu-1} e^{-(1-\mu)q^{1/\mu}}, \quad (\text{S35})$$

which for $\mu = 1/2$ can be expressed as $G(q) = D(q)/q$, where $D(q)$ is the Dawson function. The tails of $G(q)$ are like a Lorentzian $\sim 1/2q^2$ and the area is $\pi^{3/2}/2$. $G(q)$ is compared to a Lorentzian with the same tails and a Gaussian with the same FWHM and normalization in Figure S2. Notice that the distribution is not as narrow as the Lorentzian close to the central frequencies.

The resulting properties of $\mathcal{P}(\delta, T)$ are discussed in the main text.

SYSTEMATIC SCAN ACROSS A RESONANCE

A typical way to determine a resonance frequency is by observing fluorescence as the laser frequency is systematically scanned over the relevant frequencies with equal time at each point. The spectrum is reconstructed from the photo-count at each frequency. This scheme lends itself to a standard analysis relying on the CRB in a manner similar to [S5, S8]. In this section we perform such an analysis and compare the performance of a systematic scan to our stochastic protocol.

Assume first that a scan of total duration T consists in observing the fluorescence for a time $t = T/N$ at each of a set of N discrete, equally spaced frequencies $\{\delta_k\}_{k=1}^N$ on the search interval $[-\delta_{\max}, \delta_{\max}]$. A data record $D = [n_1, n_2, \dots, n_N]^T$ obtained in a time T then contains the total photo count n_k at each discrete frequency. These are independently sampled, and we assume that for large T they are normally distributed with means \bar{n}_k and variances v_k . The full data record D then samples a multivariate normal distribution $P(D|\theta) = \mathcal{N}(\boldsymbol{\mu}, \boldsymbol{\Sigma})$ with mean value vector $\boldsymbol{\mu} = [\bar{n}_1, \bar{n}_2, \dots, \bar{n}_N]^T$ and a diagonal covariance matrix with elements $\Sigma_{kk} = v_k$.

The Fisher information for estimating a parameter θ from such a distribution is well-known,

$$\mathcal{I}(\theta) = \frac{\partial \boldsymbol{\mu}^T}{\partial \theta} \boldsymbol{\Sigma}^{-1} \frac{\partial \boldsymbol{\mu}}{\partial \theta} + \frac{1}{2} \text{Tr} \left(\boldsymbol{\Sigma}^{-1} \frac{\partial \boldsymbol{\Sigma}}{\partial \theta} \boldsymbol{\Sigma}^{-1} \frac{\partial \boldsymbol{\Sigma}}{\partial \theta} \right), \quad (\text{S36})$$

yielding in this case

$$\mathcal{I}(\theta) = \sum_k \frac{1}{v_k} \left(\frac{\partial \bar{n}_k}{\partial \theta} \right)^2 + \frac{1}{2} \sum_k \left(\frac{1}{v_k} \frac{\partial v_k}{\partial \theta} \right)^2. \quad (\text{S37})$$

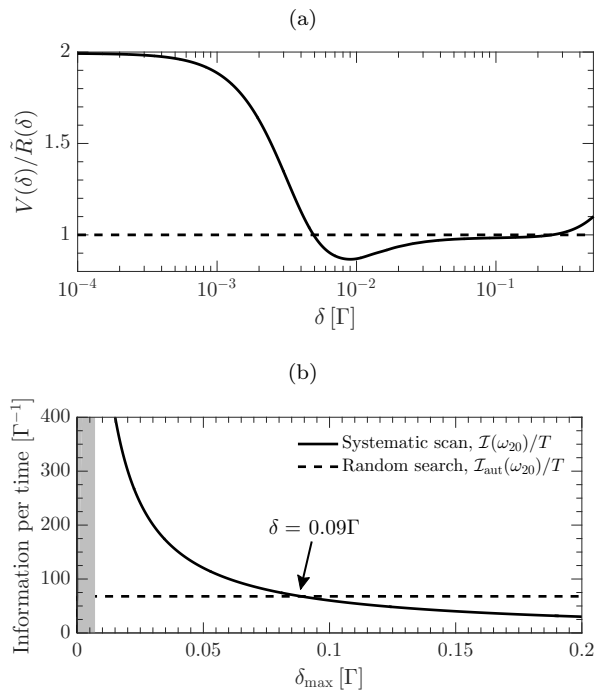


Figure S3. (a) Dependence on the detuning δ of the photo count variance per time $V(\delta)$ divided by the rate $\tilde{R}(\delta)$. The dashed line marks the Poissonian case where $V(\delta) = \tilde{R}(\delta)$. (b) Information measures for estimating ω_{20} in the Λ -system by a systematic scan and the random search protocol presented in the main text, respectively. In both cases the search is restricted to an interval $[-\delta_{\max}, \delta_{\max}]$ around the dark resonance. The shaded area is the region where $\delta_{\max} < \delta_Q$ and our statistical model of the recycling process requires modifications. Results are shown for $\Omega = 0.1\Gamma/\sqrt{2}$.

The mean and variance of the photo count at each discrete frequency follow from the master equation (S2). The mean fluorescence is $\bar{n}_k = \frac{T}{N} \tilde{R}(\delta)$. The photo count variance stems from temporal signal fluctuations, and can be expressed as

$$v_k = \bar{n}_k + 2T \sum_i \int_0^\infty d\tau \tilde{G}_i^{(2)}(\tau), \quad (\text{S38})$$

where the sum runs over the distinct emission channels and $\tilde{G}_i^{(2)}(\tau) = G_i^{(2)}(\tau) - \text{Tr}(\hat{c}_i^\dagger \hat{c}_i \rho_{\text{ss}})^2$. The last term in Eq. (S38) determines the deviation from Poissonian counting statistics.

From Eq. (S38), we notice that the last term in Eq. (S37) does not scale with T and is hence negligible at large times. Taking the limit of a continuum of frequencies, $N \rightarrow \infty$ we transform the sum in Eq. (S37) to an integral and obtain our final expression for the Fisher information of estimating a parameter θ by systematically

scanning a laser frequency across a resonance,

$$\mathcal{I}(\theta) = \frac{T}{2\delta_{\max}} \int_{-\delta_{\max}}^{\delta_{\max}} d\delta \frac{1}{V(\delta)} \left[\frac{\partial \tilde{R}(\delta)}{\partial \theta} \right]^2, \quad (\text{S39})$$

where

$$V(\delta) = \tilde{R}(\delta) + 2 \sum_i \int_0^\infty d\tau \tilde{G}_i^{(2)}(\tau) \quad (\text{S40})$$

is the frequency dependent photo count variance per time. The Fisher information Eq. (S39) leads via the Crámer Rao bound (CRB) [S2] to an uncertainty $\sigma(\theta) = [\mathcal{I}(\theta)]^{-1/2}$, which scales as $1/\sqrt{T}$ with time.

In Figure S3a we show $V(\delta)/\tilde{R}(\delta)$ as a function of the detuning δ for the Λ -system considered in the main text. Notice how the photo current exhibits photon bunching and super-Poissonian counting statistics close to the dark resonance, while it is sub-Poissonian for intermediate values and again super-Poissonian away from the resonance.

To compare with the autonomous search protocol presented in the main text, we show in Figure S3b the Fisher information Eq. (S39) for estimating ω_{20} by a systematic scan along with the equivalent information measure $I_{\text{aut}}(\omega_{20}) = (\delta_T/0.82)^2$ (see main text) of our random search for different widths of the search interval as determined by δ_{\max} . For the parameters used here, the random protocol proves superior for search intervals with $\delta_{\max} > 0.09\Gamma$.

-
- [S1] F. Bardou, J.-P. Bouchaud, A. Aspect, and C. Cohen-Tannoudji. *Lévy Statistics and Laser Cooling*. (Cambridge University Press, Cambridge, 2002).
 - [S2] J.-P. Bouchaud and A. Georges. Anomalous diffusion in disordered media: Statistical mechanisms, models and physical applications. *Physics reports*, 195(4-5):127–293, 1990.
 - [S3] E. Cinlar. Markov renewal theory. *Advances in Applied Probability*, 1(2):123–187, 1969.
 - [S4] H. Cramér. *Mathematical methods of statistics*. Princeton mathematical series No. 9 (Princeton University Press, Princeton, 1954).
 - [S5] R. J. Glauber. The quantum theory of optical coherence. *Phys. Rev.*, 130:2529–2539, Jun 1963.
 - [S6] A. H. Küllerich and K. Mølmer. Parameter estimation by multichannel photon counting. *Phys. Rev. A*, 91:012119, 2015.
 - [S7] P. Lévy. *Théorie de l'addition des variables aléatoires*, 2nd edn. (Gauthier-Villars, Paris, 2010).
 - [S8] A. Negretti, C. Henkel, and K. Mølmer. Quantum-limited position measurements of a dark matter-wave soliton. *Phys. Rev. A*, 77:043606, 2008.
 - [S9] G. Weiss. *Random Walk Theory and Applications*. (North-Holland, Amsterdam, 2010).